Supplemental Material

Thymus-derived Treg cell development is regulated by C-type-lectin–mediated BIC/miRNA155 expression

Running Title: C-type lectin regulates tTreg development

Raquel Sánchez-Díaz[a,e], Rafael Blanco-Dominguez[a], Sandra Lasarte[a,e], Katerina Tsilingiri[a], Enrique Martín-Gayo[b], Beatriz Linillos-Pradillo[a] Hortensia de la Fuente[c,e], Francisco Sánchez-Madrid[c,e], Rinako Nakagawa[d], María L. Toribio[b], & Pilar Martín[a,e].

[a]Signaling & Inflammation Program, Centro Nacional de Investigaciones Cardiovasculares (CNIC), Madrid, Spain, 28029.

[b]Centro de Biología Molecular Severo Ochoa, Consejo Superior de Investigaciones Científicas, Universidad Autónoma de Madrid, Spain., 28049.

[c]Department of Immunology, Hospital de La Princesa, Madrid, Spain, 28006.

[d]Immunity and Cancer Laboratory, The Francis Crick Institute, London, WC2A 3LY, UK

[e]CIBER CV, Instituto de Salud Carlos III, Spain, 28029.

Corresponding author. Pilar Martin. Tel: +34 914531200; Email: pmartinf@cnic.es

The PDF file includes:

Supplemental Figure S1. CD69 is required for Foxp3^{+} pTregs homeostasis in secondary lymphoid organs.

Supplemental Figure S2. The use of anti-Foxp3 antibodies is not as accurate as the use of Foxp3 reporter mice.

Supplemental Figure S3. Reduced levels of Foxp3-mRFP^{+} Treg cells in the blood of chimeric mice reconstituted with *cd69*$^{-/-}$ precursors.

Supplemental Figure S4. CD69^{+} hematopoietic stem cells are more prone to develop tTregs after reconstitution.

Supplemental Figure S5. CD69^{+} hematopoietic stem cells are more prone to develop pTregs after reconstitution.

Supplemental Figure S6. Scheme depicting FACS sorting strategy to isolate CD69+ and CD69- Foxp3-reporter tTreg cells**.**

Supplemental Figure S7. Expression of P-Stat5, miR-155 and SOCS-1 target protein in Spleen CD69^{+} or CD69^{-} Treg cells.

Supplemental Figure S8. Expression of miR-155 and target proteins in the absence of Jak3-STAT5 signaling pathway.

Supplemental Figure S9. Signaling downstream CD69 up-regulates miR-155 expression in a positive feedback loop.

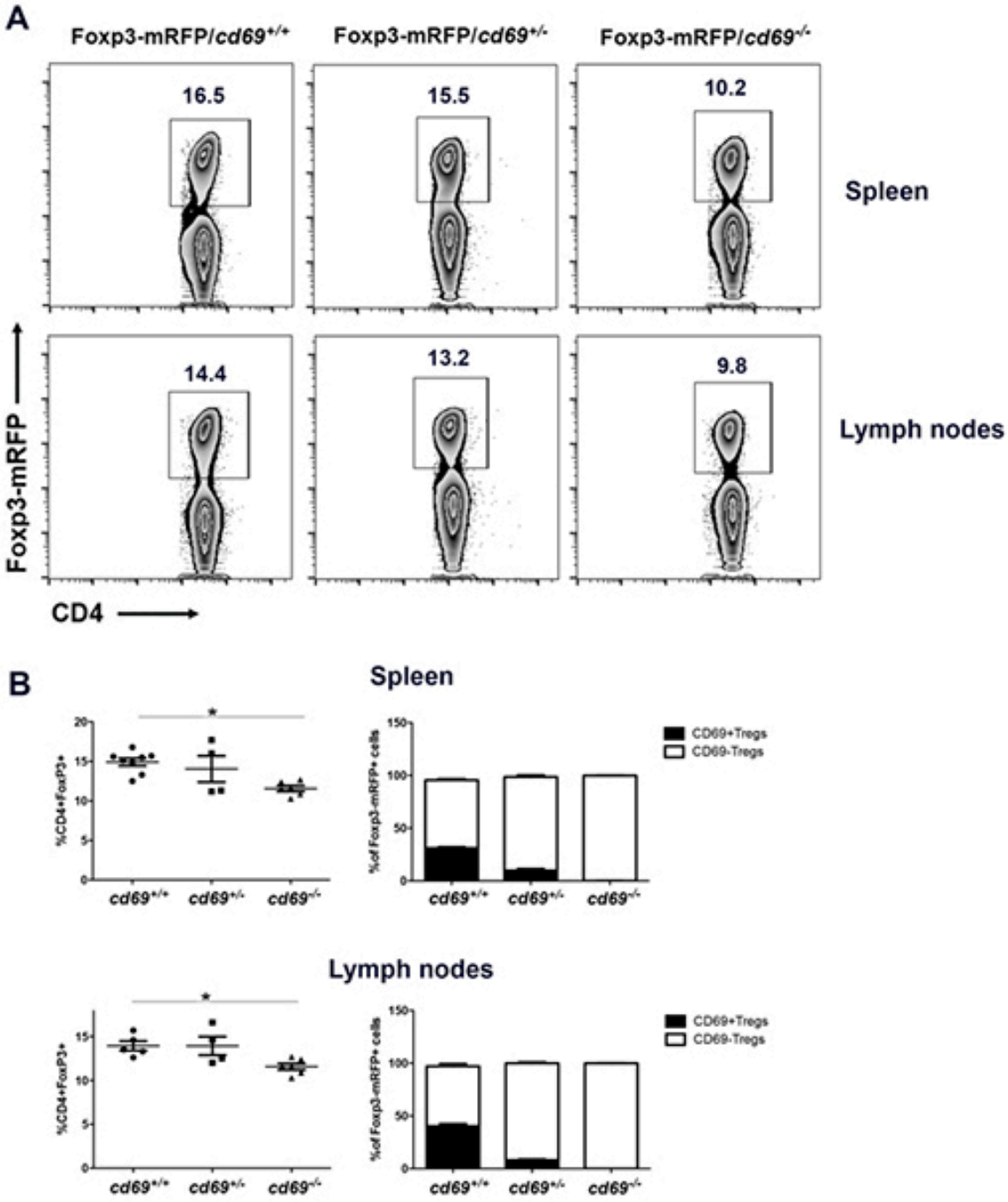

Supplemental Figure S1. CD69 is required for Foxp3$^+$ pTregs homeostasis in secondary lymphoid organs. (A) Flow cytometry analysis of CD4$^+$ Foxp3$^+$ Tregs in cells isolated from spleens and peripheral lymph nodes from *cd69*$^{+/+}$, *cd69*$^{+/-}$, and *cd69*$^{-/-}$ littermates bearing a Foxp3-mRFP reporter gene, of 8 to 12 weeks of age. (B) *Left*, percentages of gated CD4$^+$ Foxp3$^+$ Tregs in spleen and lymph nodes from adult reporter littermates. *Right*, The bar chart shows the percentage (± S.D.) of CD69$^+$ (black) and

CD69$^-$ (white) pTregs within the spleen or lymph nodes of the indicated *reporter* mice. Data are from at least 7 litters with 3 to 12 littermates each as in Figure 1. Error bars show S.D. Data were evaluated by ANOVA followed by Bonferroni's multiple comparison test: * $P < 0.05$.

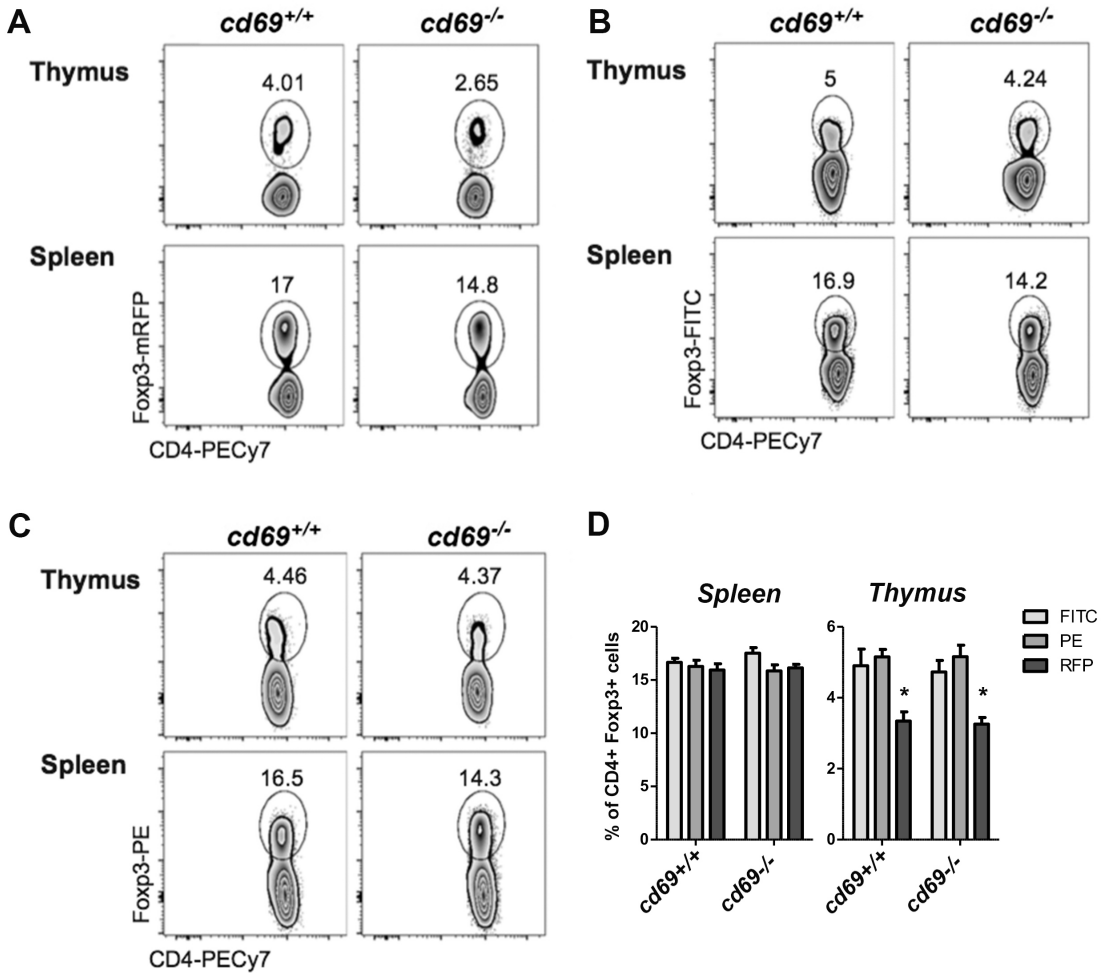

Supplemental Figure S2. The use of anti-Foxp3 antibodies is not as accurate as the use of Foxp3 reporter mice. We performed Foxp3 staining with two different tags in thymus and spleens from Foxp3-mRFP mice. Thymus and spleens from Foxp3-mRFP/*cd69*$^{+/+}$ and Foxp3-mRFP/*cd69*$^{-/-}$ mice were harvested and stained with CD4-PeCy7 alone (A) or together with anti-Foxp3-FITC (B) or –PE (C). The percentage of Foxp3^{+} cells was analyzed in different emission channels after the acquisition of the data by FACS (LSR Fortessa BD), after excitation with the different wavelength. (D) Comparison of Foxp3 signals in CD4^{+} T cells. Data were evaluated by ANOVA followed by Bonferroni's multiple comparison test: * $P < 0.05$.

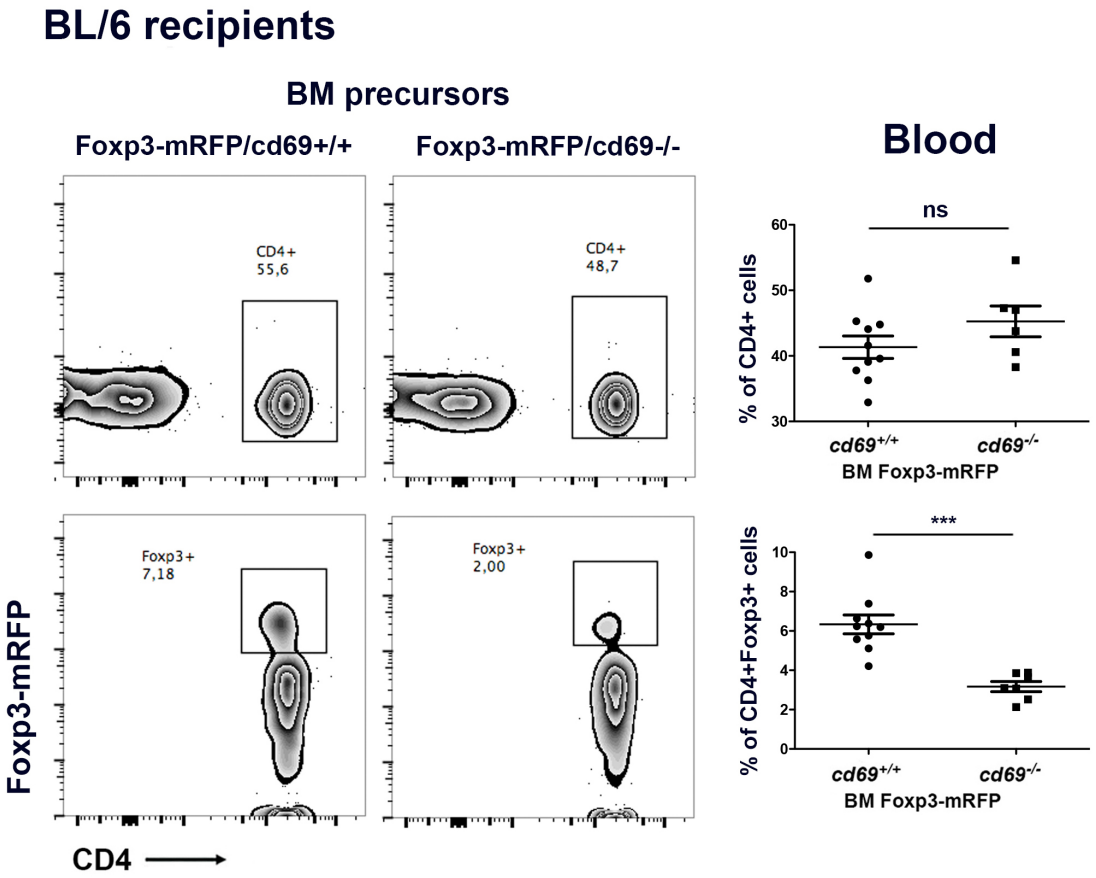

Supplemental Figure S3. Reduced levels of Foxp3-mRFP$^+$ Treg cells in the blood of chimeric mice reconstituted with *cd69*$^{-/-}$ precursors. Eight-twelve-week-old C57BL/6 recipient mice received two split doses of 6.5 Gy -radiation, and were i.v. injected with bone marrow cells from Foxp3-mRFP/*cd69*$^{+/+}$ or Foxp3-mRFP/*cd69*$^{-/-}$ littermates. After at least 10 weeks, the contribution of the different donor bone marrow precursors to blood circulating Tregs was determined by FACS. *Left*, representative dot plots. *Right*, percentages of gated CD4$^+$ T cells and CD4$^+$Foxp3$^+$ tTregs in the blood of chimeric mice. Dot represent individual mice. All data are representative of at least 3 independent experiments with at least 3 recipient mice per group. Error bars show S.D. *** $P < 0.001$ (Student's t-test). ns; non significant.

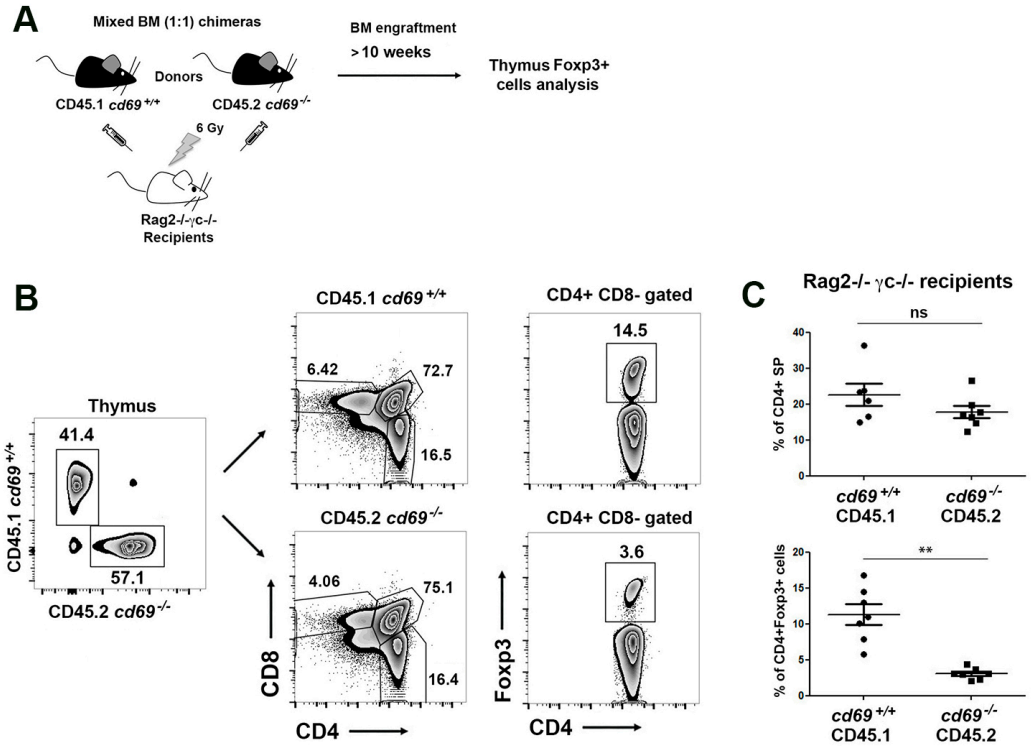

Supplemental Figure S4. CD69^{+} hematopoietic stem cells are more prone to develop tTregs after reconstitution. (A) Ten-week-old Rag2$^{-/-}$ γc$^{-/-}$ recipient mice received 6,5 Gy γ-radiation and were i.v. injected with a mixture of CD45.1- *cd69*$^{+/+}$ or CD45.2- *cd69*$^{-/-}$ bone marrow precursors at a ratio of 1:1. (B) The contribution of the different donor bone marrow precursors to tTreg cells development was determined by FACS. (C) Percentages of gated CD4^{+} SP cells and CD4^{+}CD8^{-}Foxp3^{+} tTregs within CD45.1 or CD45.2 donors in the thymus. All data are representative of at least 3 independent experiments with at least 3 recipient mice per group. Error bars show S.D. * P < 0.05, ** P < 0.01, *** P < 0.001 (Student's t-test).

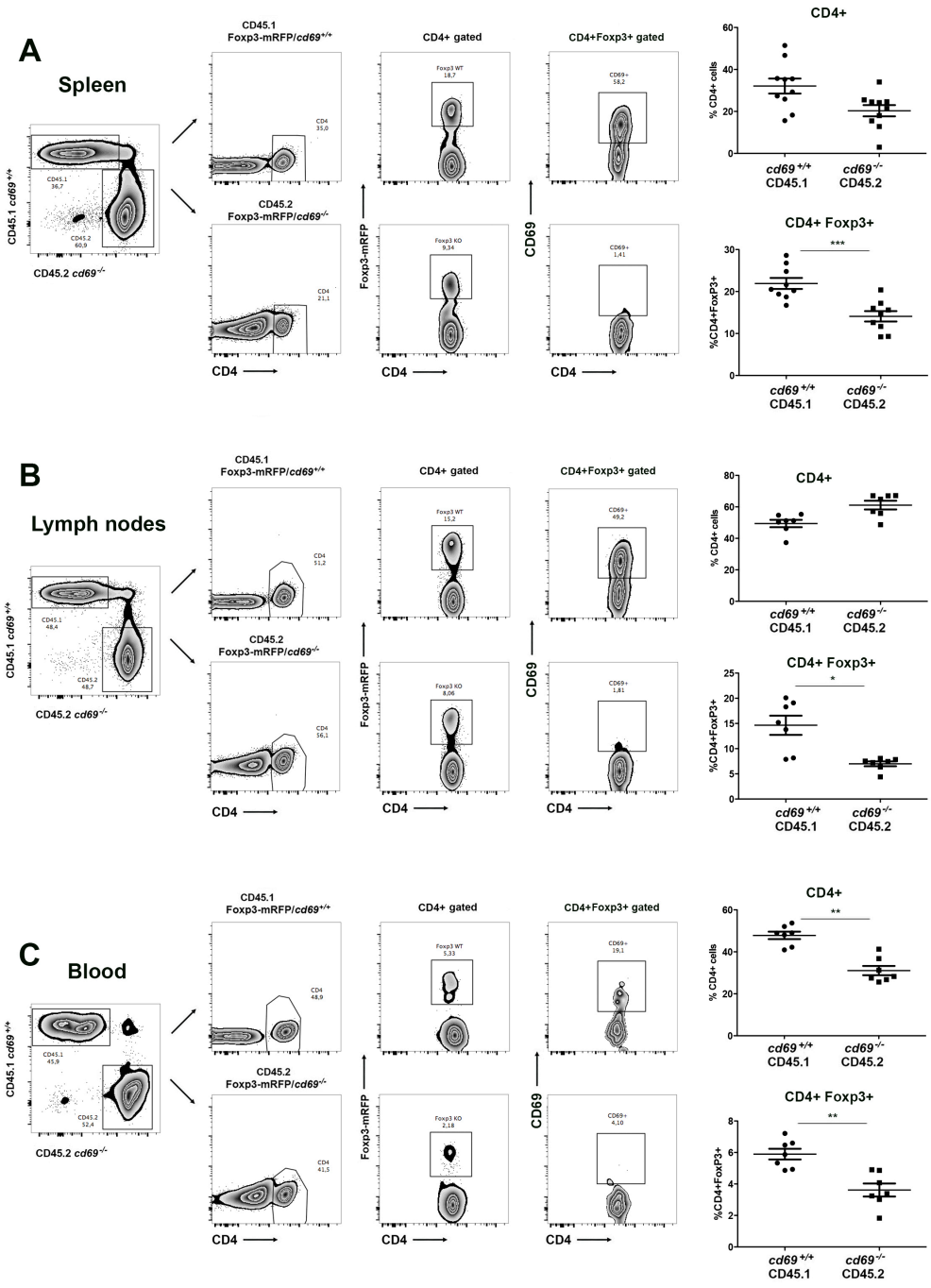

Supplemental Figure S5. CD69^{+} hematopoietic stem cells are more prone to develop pTregs after reconstitution. Ten-week-old Rag2$^{-/-}$ γc$^{-/-}$ recipient mice received 6,5 Gy γ-radiation and were i.v. injected with a mixture of CD45.1- *cd69*$^{+/+}$ or CD45.2- *cd69*$^{-/-}$ bone marrow precursors at a ratio of 1:1. The contribution of the different donor bone marrow precursors to pTreg cells development in spleen (A),

lymph nodes (B) and blood (C). Percentages of gated $CD4^+$ cells and $CD4^+Foxp3^+$ pTregs within CD45.1 or CD45.2 donors in the different tissues and CD69 expression in pTregs were determined by FACS. All data are representative from 10 recipient mice. Error bars show S.D. * $P < 0.05$, ** $P < 0.01$, *** $P < 0.001$ (Student's t-test).

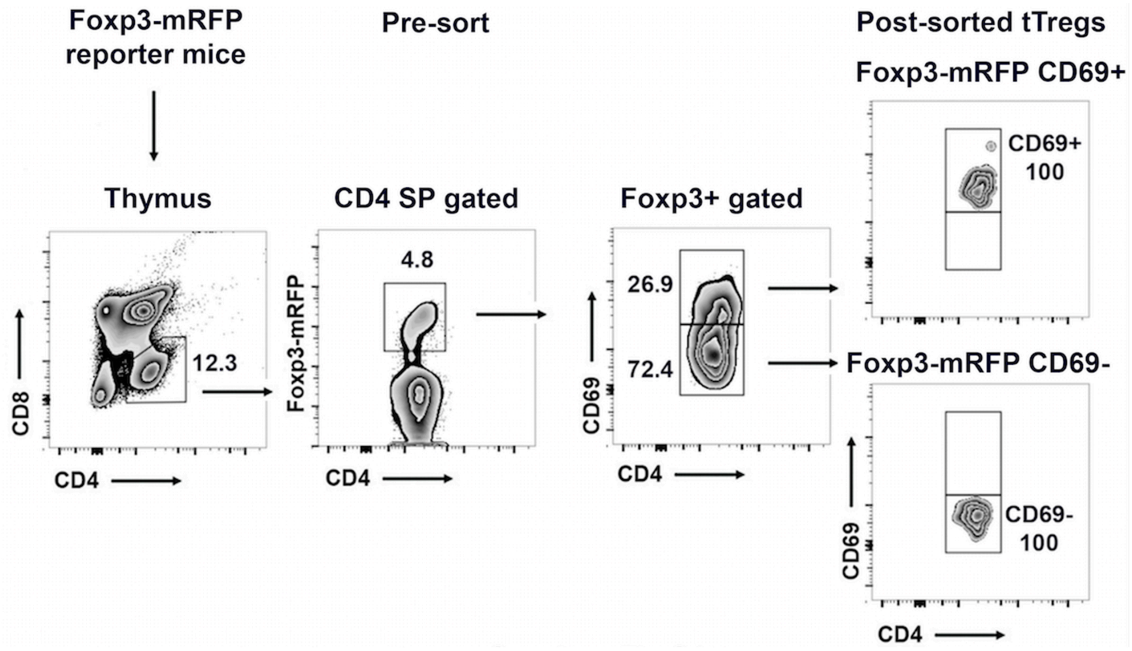

Supplemental Figure S6. Scheme depicting FACS sorting strategy to isolate CD69+ and CD69- Foxp3-reporter tTreg cells. Cells were isolated from the thymus of *cd69*$^{+/+}$/Foxp3-mRFP reporter mice, and stained with CD4 and CD69 antibodies. CD4^{+}CD8^{-}Foxp3^{+} cells were sorted based on the levels of CD69 expression. Sorted cells were used for FACS, qPCR and WB analysis. Gates and arrows indicate the sorting strategy. Numbers indicate the percentage of cells within the gates.

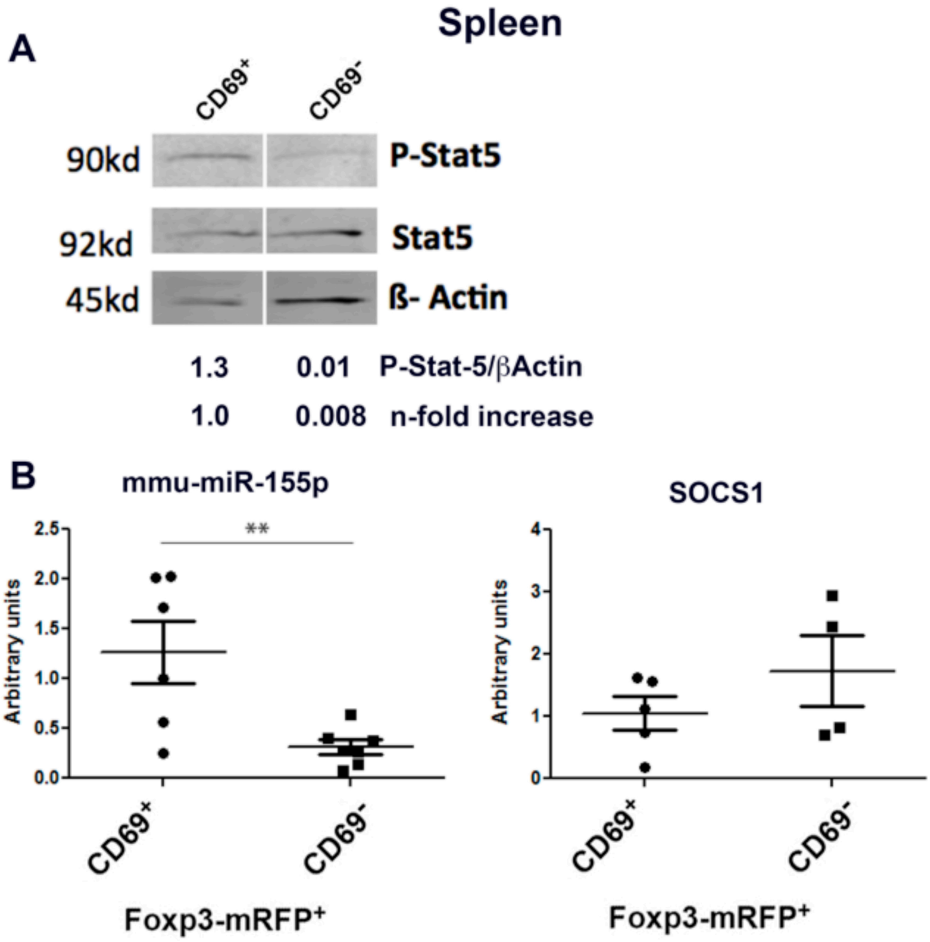

Supplemental Figure S7. Expression of P-Stat5, miR-155 and SOCS-1 target protein in Spleen CD69$^+$ or CD69$^-$ Treg cells.

(A) Representative WB showing the levels of STAT5 phosphorylation in Tregs sorted from spleens of *cd69*$^{+/+}$/Foxp3-mRFP reporter mice, and stained with CD4 and CD69 antibodies. Phosphorylation levels are normalized to STAT5 and β actin total protein levels. (B) q-PCR analysis of the relative expression of mmu-miR155 and SOCS1 in CD69$^+$ and CD69$^-$ spleen sorted Tregs. Expression was normalized to the levels in CD69$^+$ tTregs. Data were analyzed by t-test. All data are derived from at least 5 independent sortings/experiments (3 animals per sorting). Error bars show S.D. ** $P < 0.01$ (Student's t-test).

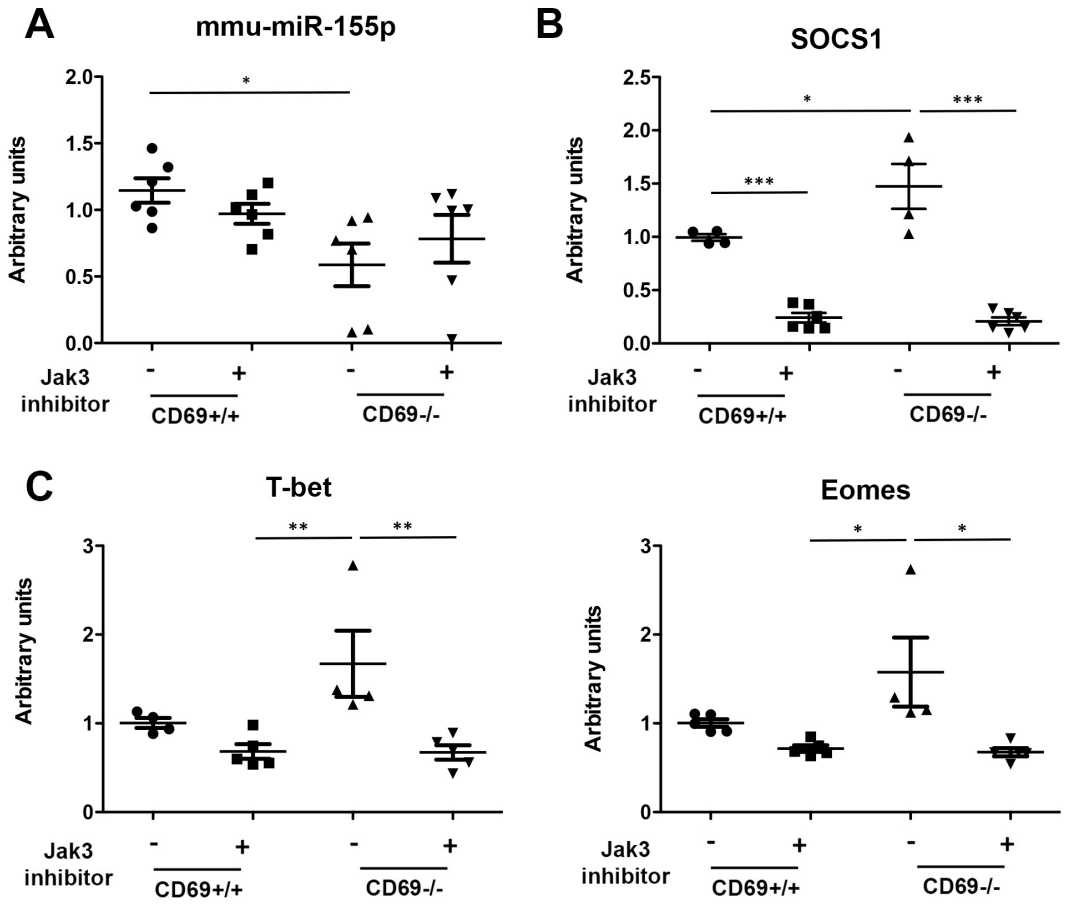

Supplemental Figure 8. Expression of miR-155 and target proteins in the absence of Jak3-STAT5 signaling pathway. Naïve $CD4^+$ T cells from Foxp3-mRFP/*cd69*$^{+/+}$ or Foxp3-mRFP/*cd69*$^{-/-}$ littermates were cultured for 72 hours under Treg-skewed conditions and treated with a chemical Jak3 inhibitor or an equal concentration of DMSO for the last 9 hours. q-PCR analysis of the relative expression of mmu-miR155 (A), SOCS1 (B), T-bet and Eomes (C) in *cd69*$^{+/+}$ or *cd69*$^{-/}$ inducible Tregs in the presence of Jak3 inhibitor when indicated. Expression was normalized to the levels in *cd69*$^{+/+}$ inducible Tregs with-out Jak3 inhibitor. Data are from two independent experiment (n=3 from each genotype). Error bars show S.D. Data were evaluated by ANOVA followed by Bonferroni's multiple comparison test: * $P < 0.05$, ** $P < 0.01$, *** $P < 0.001$.

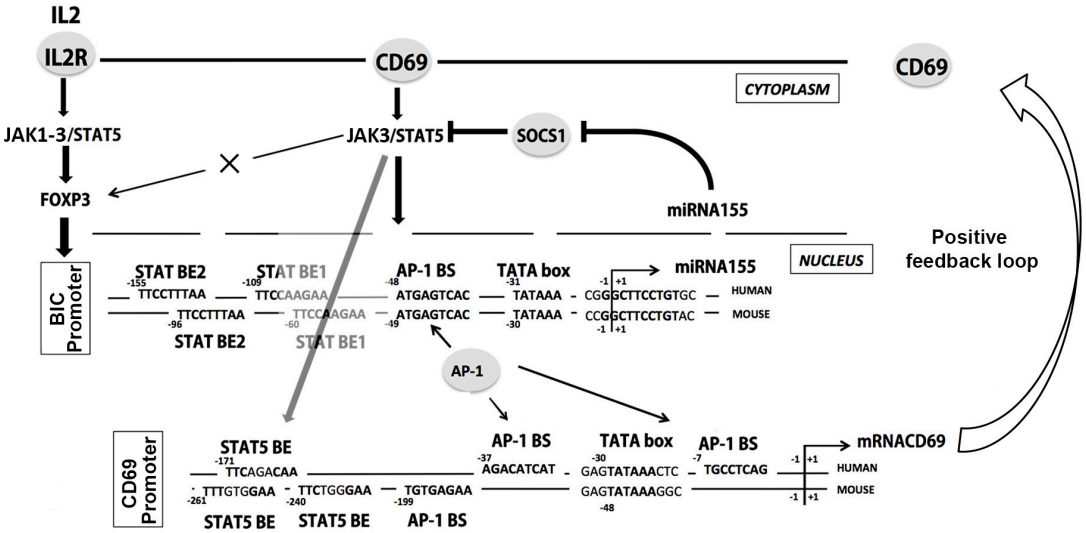

Supplemental Figure 9. Signaling downstream CD69 up-regulates miR-155 expression in a positive feedback loop. Concomitant CD69 and IL-2R signaling in the regulation of miR-155. Conserved sequences for human and mouse BIC and CD69 promoters have been obtained from GenBank (*Mus musculus* BIC noncoding mRNA GenBank: AY096003.1; *Homo sapiens* (human) MIR155 host gene GenBank: NC_018932.2; *Mus musculus* CD69 antigen GenBank: NC_000072.6; *Homo sapiens* CD69 molecule GenBank: NC_000012.12). The BIC/miR-155 and CD69 promoter sequences share a similar organization of STAT5 and AP-1 binding elements, with 2 putative STAT binding elements located upstream of the TATA box and AP-1 element. The consensus sequences for STAT and AP-1 binding sites are shown both in mice and human promoters of CD69 and BIC. Numbers indicate the position regarding the starting codon ATG within each promoter.